

Analysis of Strain-induced Pockels effect in Silicon

C. L. Manganelli ¹, P. Pintus ¹, C. Bonati ², F. Di Pasquale ¹

1. Scuola Superiore Sant'Anna, via G. Moruzzi 1-Pisa
2. INFN-Sezione di Pisa-Largo Pontecorvo 3-Pisa

*Corresponding author: costanza.manganelli@sssup.it

Abstract:

The recently discovered Pockels effect in strained silicon has made silicon a promising candidate material for optical modulators and switches. In this paper we investigate the electro-optic effect induced by applied strain gradient in silicon optical waveguides. We also propose a model that simplifies the description of the electro-optic effect in strained silicon providing a tool for design and optimization of optical devices.

Keywords: Pockels effect, strain gradient, silicon, electro-optic material.

1. Introduction

The electro-optic effect consists in the change of the refractive index induced by an electric field that varies slowly compared with the frequency of an optical signal. In the particular case of the Pockels effect, also called linear electro-optic effect, the change in the refractive index is proportional to the applied electric field, providing an efficient physical mechanism for optical modulation. However, a peculiarity of the Pockels effect is that it arises only in crystalline solids lacking of inversion symmetry. As a consequence, for centrosymmetric crystals (like silicon) the Pockels effect can be observed only when the inversion symmetry is broken, e.g., by the presence of significant surface/interface effects or by an inhomogeneous mechanical stress. In this work, we propose a model that links the electro-optic effect to the applied strain (in fact to the strain gradient). This model essentially relies on symmetry arguments and can be seen as a coherent formalization of some intuitive ideas present in the literature and relating the effective susceptibility to the strain gradient.

2. Theory

2.1 Polarization vector and Pockels effect

The quadratic nonlinear susceptibility is conventionally defined, for a local and causal

medium, by the following relation between the (quadratic component of the) polarization vector $P_i^{(2)}(t)$ and the electric field $E(t)$:

$$P_i^{(2)}(t) = \epsilon_0 \iint_0^\infty \chi_{ijk}^{(2)}(\tau_1, \tau_2) E_j(t - \tau_1) E_k(t - \tau_2) d\tau_1 d\tau_2 \quad (1)$$

where ϵ_0 is the free-space dielectric permittivity and $\chi_{ijk}^{(2)}$ is the susceptibility tensor. In the frequency domain the same formula can be rewritten in the following way:

$$P_i^{(2)}(\omega_1, \omega_2) = \epsilon_0 \chi_{ijk}^{(2)}(\omega_1 + \omega_2, \omega_1, \omega_2) E_j(\omega_1) E_k(\omega_2) \quad (2)$$

The Pockels effect consists in the variation of the index of refraction at frequency ω when a static electric field is applied. In the case of Pockels effect, the definition of polarization vector becomes:

$$P_i^{(2)}(\omega) = 2 \epsilon_0 \chi_{ijk}^{(2)}(\omega; \omega, \mathbf{0}) E_j(\omega) E_k(0) \quad (3)$$

where the factor 2 derives from inversion symmetry on the $\chi_{ijk}^{(2)}$ tensor.

2.2 The strain-induced Pockels effect

In the linear theory of elasticity, a small deformation $\mathbf{x} \rightarrow \mathbf{x} + \mathbf{u}(\mathbf{x})$ is described by the symmetric strain tensor ϵ , defined by

$$\epsilon_{ij} = \frac{\partial u_i}{\partial x_j} + \frac{\partial u_j}{\partial x_i} \quad (4)$$

where $\mathbf{u}(\mathbf{x})$ represents the displacement of a material point. In order to determine the relation between $\chi^{(2)}$ and ϵ , the following strategy has been identified: the most general expression compatible with the symmetries of the problem is considered, then the various possible terms are classified according to their “strength” retaining only the most relevant ones. The final relation will depend on a number of unknown constants, which have to be identified by comparing with experimental data.

As a starting point we assume that $\chi^{(2)}$ is a local functional of ϵ , i.e. that $\chi^{(2)}$ at point \mathbf{x} depends only on the values of ϵ and its derivatives at \mathbf{x} . We then assume that this dependence is analytic and we

develop everything in Taylor series, thus arriving to the following expression:

$$\chi_{ijk}^{(2)} = \left. \frac{\partial \chi_{ijk}^{(2)}}{\partial \zeta_{\alpha\beta\gamma}} \right|_{\varepsilon=0} \zeta_{\alpha\beta\gamma} \quad (5)$$

where $\zeta_{\alpha\beta\gamma} = \partial \varepsilon_{\alpha\beta} / \partial x_\gamma$ is the strain gradient tensor and, as a consequence, in a more compact notation, we can write that:

$$\chi_{ijk}^{(2)}(x, \omega_1 + \omega_2; \omega_1, \omega_2) =$$

$$T_{ijk\alpha\beta\gamma}(\omega_1 + \omega_2; \omega_1, \omega_2) \zeta_{\alpha\beta\gamma}(x) \quad (6)$$

The tensor T inherits some symmetries from ε : it is symmetric for $\alpha \leftrightarrow \beta$ and, as far as the Pockels effect is concerned, for $i \leftrightarrow j$ if a lossless medium is considered [5,6]. It is worth noting that only 324 of the $3^6 = 729$ components of T are linearly independent. Since T is an invariant tensor for the lattice symmetry, this number can be further largely reduced. In the case of the lattice octahedral symmetry typical of the silicon crystal, we proved that the number of independent components is in fact only 15.

In the most common devices designed to give an estimation of the Pockels effect (see e.g. Fig 1), the static electric field is directed along the y direction; as a consequence, the final expression for the effective dielectric susceptibility is given by:

$$\chi_y^{eff}(\omega) = c_i o_i(\omega) \quad (7)$$

where the coefficients c_i ($i = 1, \dots, 15$) are the independent entries of the tensor T and the terms o_i are linear combinations of the weighted strain gradients $\overline{\zeta_{\alpha\beta\gamma}^{ij}}(\omega)$ that are defined as

$$\overline{\zeta_{\alpha\beta\gamma}^{ij}}(\omega) = \frac{\varepsilon_0 c n^{eff}}{N} \int E_i^*(x) \zeta_{\alpha\beta\gamma}(x) E_j(x) dA \quad (8)$$

where ε_0 is the free-space dielectric permittivity, c is the speed of light in the vacuum, $E_i^*(x)$ and $E_j(x)$ are the components of the optical field and n^{eff} is the effective index of the mode. In order to clarify the role played by the electromagnetic field in the estimation of the effective index, the analytical expression of the normalization factor N is

$$N = \frac{1}{2} \int (\mathbf{E} \times \mathbf{H}^* + \mathbf{E}^* \times \mathbf{H}) \cdot \mathbf{i}_z dA \quad (9),$$

where E and H are the components of electric and magnetic fields and A is the waveguide cross section. The linear combinations of the weighted strain gradients $\overline{\zeta_{\alpha\beta\gamma}^{ij}}(\omega)$ will be called overlap function and reported with the simpler notation of o_i that will be clarified in the appendix.

2. Experimental setup

The strain induced electro-optic effect of silicon has been measured by exploiting a fully integrated Mach Zehnder Interferometer in a push-pull configuration with a difference length. The strain is applied by covering the silicon waveguide with a straining silicon nitride (Si_3N_4) cladding layer and the effective index variation is measured from the spectral wavelength shift at the MZI-output as a function of the applied voltage. For the electro-optic characterization, a variable electrostatic field is applied to the MZI arms by changing the voltage from -30 V to 30 V.

The waveguide cross-section used in [1,2] is schematically shown in Fig. 1. A silicon rib waveguide was manufactured on a silicon-on-insulator (SOI) substrate with a 220 nm thick (100)-oriented top silicon layer over a 3 μm thick buried oxide. Silicon waveguides are fabricated by an etching process that leaves a slab thickness of 45 nm. A 350 nm thick Si_3N_4 layer is deposited using remote plasma enhanced chemical vapor deposition and after the annealing process, a protective SiO_2 cladding layer is deposited on the top (850 nm thick).

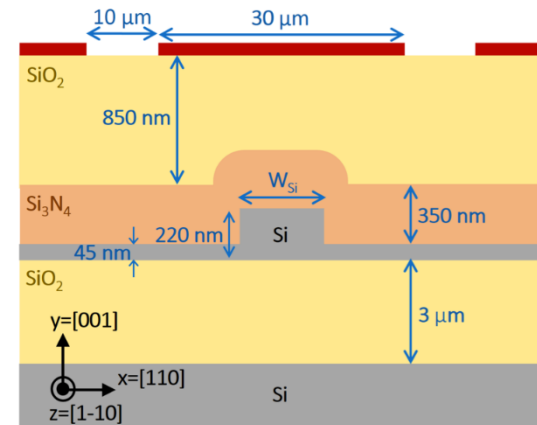


Figure 1. Slab waveguide cross-section described in [1].

3. Use of COMSOL Multiphysics

In order to investigate the validity of our model, we need to evaluate the strain gradient for the structures described in the previous section. Since silicon elastic properties significantly depend on the orientation of the crystalline structure, they have been taken into account in the mechanical simulation. To describe the deformation of silicon, one possibility could be to make use of the Hooke's law, i.e. the linear relation between strain and stress, which for materials with cubic symmetry involves only three independent components. A more convenient description, that avoids tensorial transformation, is however the one that makes use of the orthotropic model. A material is said to be orthotropic when it has at least two orthogonal planes of symmetry. Its elasticity can be described by a matrix that takes into account the fundamental elasticity quantities in the axes of interest: the Young's module (Y), the Poisson's ratio (ν) and the shear modulus (G). The most common use of orthotropic expressions for silicon is to provide the elasticity values in the frame of a standard (100)-silicon wafer. When $z=[1-10]$, $x=[110]$ and $y=[001]$ like in the device investigated in [1] the elasticity moduli are [3] :

$$Y_x = 169 \text{ GPa}, Y_y = 130 \text{ GPa}, Y_z = Y_x$$

$$\nu_{xy} = 0.36, \nu_{yz} = 0.28, \nu_{xz} = 0.064$$

$$G_{xy} = 79.6 \text{ GPa}, G_{xz} = 50.9 \text{ GPa}, G_{yz} = G_{xz} \quad (10).$$

The deformation of the silicon waveguides has been computed by using COMSOL multiphysics tools. Assuming 1 GPa compressive stress as the initial condition for the silicon nitride layer, the elastic strain has been computed for the structure in Fig 1. For the silicon waveguide and the buried silicon we used the values of the elastic modulus, the shear modulus and the Young's modulus in [3]. Since for the solid analysis a 2D model has been considered, the components ϵ_{xz} and ϵ_{yz} of the strain identically vanish. For the same reason, the derivative of the strain coefficient with respect to z are assumed to be zero (see Fig. 2).

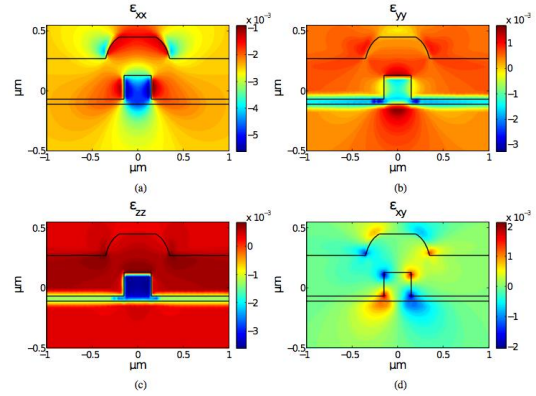


Figure 2. Simulated strain tensor components for the waveguide cross section in in ref .[1]

The results of the electromagnetic mode analysis, performed using COMSOL are shown in Fig. 3 for the device described in Fig. 1. The waveguides show a single mode behavior but E_z and E_y components are not negligible compared to E_x component and thus the mode is clearly not purely transverse electric. The high value of E_z is due to the high index step of the waveguide.

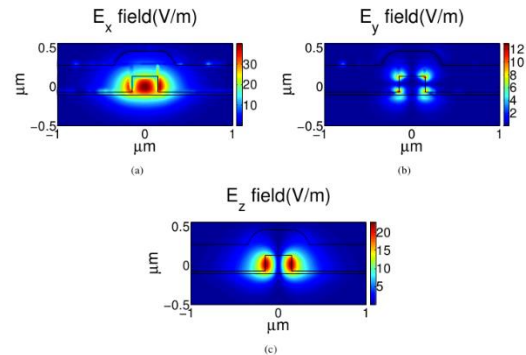


Figure 3. Electromagnetic fields components in ref. [1]

Combining the results of the electromagnetic mode analysis with the solid mechanics results, the overlap integrals have been computed for the structure in Fig. 1. Results are shown in Fig. 4 and their analytic value are reported in the appendix. Note that Fig. 4 only reports the largest overlap factors; the others are orders of magnitude smaller and then not significant for design optimization. Having computed these overlap functions for the selected experimental setup, the c_i coefficients of eq. 7 can be estimated by fitting the experimental data, providing, in this way a big breakthrough in silicon photonic for the optimization of optical devices.

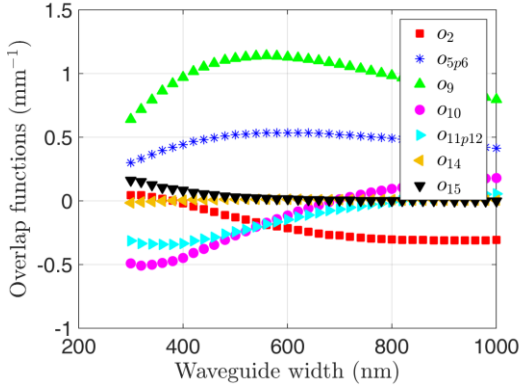


Figure 4. Overlap functions in ref [1,4].

8. Conclusions

In this paper we present an investigation through COMSOL multiphysics of a novel model that describes the strain-induced dielectric susceptibility in centro-symmetric crystals. We underlined that the combination of optical modes and mechanical stress analysis is required in order to have an accurate description of second order-dielectric susceptibility. The main result of our analysis consists in a simple relation between the second order dielectric susceptibility and linear combinations of weighted strain gradient tensor. The future presence of accurate experimental data will give us the possibility of evaluating a few parameters that will allow design and optimization of electro-optic modulators.

9. References

1. B. Chmielak, et. al., "Investigation of local strain distribution and linear electro-optic effect in strained silicon waveguides," *Opt. Express*, **21**, (2013).
2. B. Chmielak, et. al., "Pockels effect based fully integrated, strained silicon electro-optic modulator," *Opt. Express*, **19**, (2011).
3. M. A. Hopcroft, et. al., "What is the Young's modulus of silicon?," *IEEE Journal of Microelectromechanical Systems*, **19**, (2010).
4. C. L. Manganelli, P. Pintus, C. Bonati, "Modeling of Strain-induced Pockels effect in Silicon," arXiv:1507.06589 [physics.optics].
5. L. Landau et. al., "Electrodinamic of Continuous Media," Elsevier Butterworth Heinemann, 1984.
6. A. Yariv et. al., "Optical waves in crystals", A

10. Acknowledgements

This work is partially supported by the Italian Ministry of Education, University and Research (MIUR) through the FIRB project "MINOS". The authors would like to thank Martino Bernard, Massimo Borghi, Mattia Mancinelli, and Lorenzo Pavesi from University of Trento; Mher Ghulinyan, Georg Pucker from Fondazione Bruno Kessler; Nicola Andriolli, Isabella Cerutti and Koteswararao Kondepudi from Scuola Superiore Sant'Anna.

11. Appendix

The overlap functions in the main text are computed with respect to the coordinate frame shown in Fig. 1 and their explicit form is reported in the following:

$$\begin{aligned}
 o_1 &= \overline{\zeta_{yyy}^{yy}}, & o_2 &= \overline{\zeta_{yyy}^{zz}} + \overline{\zeta_{yyy}^{xx}}, \\
 o_3 &= \text{Re} \left\{ \overline{\zeta_{yyy}^{zz}} + \overline{\zeta_{yyy}^{xx}} \right\}, \\
 o_4 &= \overline{\zeta_{xxy}^{yy}} + \overline{\zeta_{xxy}^{xx}}, \\
 o_5 &= \frac{1}{2} \left\{ \overline{\zeta_{xxy}^{xx}} + \overline{\zeta_{xxy}^{zz}} + \overline{\zeta_{xxy}^{zz}} + \overline{\zeta_{xxy}^{xx}} \right\}, \\
 o_6 &= o_5, & o_7 &= o_3 \\
 o_8 &= 2\text{Re} \left\{ \overline{\zeta_{yyx}^{xy}} \right\}, \\
 o_9 &= \overline{\zeta_{xxy}^{xx}} + \overline{\zeta_{xxy}^{zz}} - \overline{\zeta_{xxy}^{zz}} - \overline{\zeta_{xxy}^{xx}}, \\
 o_{10} &= 2 \left\{ \overline{\zeta_{xyx}^{xx}} - \overline{\zeta_{xyx}^{zz}} \right\}, \\
 o_{11} &= \overline{\zeta_{xyx}^{xx}} - \overline{\zeta_{xyx}^{zz}}, & o_{11} &= o_{12} \\
 & & o_{13} &= 2 \overline{\zeta_{xyx}^{yy}} \\
 o_{14} &= 2\text{Re} \left\{ \overline{\zeta_{xxx}^{yx}} - \overline{\zeta_{xxx}^{yx}} \right\}, \\
 o_{15} &= 4\text{Re} \left\{ \overline{\zeta_{xyy}^{yx}} \right\} \quad (11).
 \end{aligned}$$